

# WOUND ROLL STRESS ANALYSIS INCLUDING AIR ENTRAINMENT AND THE FORMATION OF ROLL DEFECTS

by

A. W. Forrest Jr.

DuPont  
Circleville, Ohio, U.S.A.

## ABSTRACT:

Numerous procedures have been developed to determine the stresses inside wound rolls of film. These typically use factors such as winding tension, film thickness and film properties to calculate the stresses. The calculation presented here includes provisions for entrained air and methods to predict the formation of common roll defects. The entrained air pressure, the air gap and the winding tension are used to fully define the surface boundary condition during winding. Incipient buckling criteria are developed to predict deformations induced by transverse and circumferential stresses. The results include radial pressures, circumferential and transverse direction stresses, buckling defect formation indicators and the entrapped air pressure for the plane-strain case.

## NOMENCLATURE

C	Constant
D	Flexural rigidity ( $ET^3/12(1-\mu^2)$ ), PA mm <sup>3</sup>
e	Strain
E	Elastic Modulus, Pa
F	Force on a single sheet in the plane of the film, N
$h_1$	Air gap at roll surface, mm
$h_0$	Maximum asperity height, mm
K	Radial support stiffness for sheets in rolls, Pa/m
$K_1$	First stack compression coefficient, Pa
$K_2$	Second stack compression coefficient
n	Number of wraps in surface layer
P	Pressure in wound roll of film, Pa
$P_1$	Atmospheric pressure, Pa
q	Radial displacement in winding roll, mm

r	Radial direction in roll
R	Outer radius of wound roll, mm
R <sub>c</sub>	Outer radius of core, mm
R <sub>ci</sub>	Inner radius of core, mm
S	Stress in wound roll of film, Pa
s	Length along film surface, mm
T	Winding tension in film, Pa
y	Normal displacement of film due to buckling, mm
δ	Incremental value of a parameter
Γ	Wavelength of buckles as defined on Fig 2
μ	Poisson's ratio

### Subscripts

c	Core condition
r	Radial direction
t	Relating to film tension
z	Transverse or z direction
θ	Circumferential direction

## INTRODUCTION

There are a number of existing stress analyses for wound rolls of film [1-4]. These procedures provide a means of calculating the stresses in wound rolls under certain conditions. They use the film tension as the primary boundary condition at the surface of the winding rolls. No attempt has been made, however, to include the effect of air entrainment in the calculations. It is well known that air is wound into the rolls between the layers of film and that this can have a dramatic effect on the roll formation. With the development of calculations that determine the air pressure and gap thickness at the roll surface [5], a procedure is needed to include this information as a part of the boundary conditions for the roll stress calculation and provide air pressure predictions inside wound rolls.

Using the results from most roll stress calculations also presents a problem. It has been known [6,7] for some time that many of the film defects are buckles. To use the roll stresses, we need to develop buckling criteria that can be used to determine whether or not buckles can occur in the wound rolls. These types of defects are more prevalent in wide rolls of film where the plane-stress assumption normally used does not apply. A calculation that uses the plane-strain assumptions for roll stress and includes buckling criteria is needed.

This work extends the capabilities of the roll stress calculation procedure to include these needed additions. It includes the plane-strain calculation of the roll stresses in the radial, circumferential and axial directions. Calculations are included to determine if the film will form defects related to buckles from circumferential or axial compression. The pressure of the air trapped between layers of film also is determined. It requires stack compression data for the film to determine the radial stiffness and normal film properties in the other directions. Since the entrained air is handled separately, the stack compression data should be obtained from tests in a vacuum (see

Reference [8]). The conditions at the surface are described by both tension and entrained air pressure tables.

## THE FORMATION OF RIDGES OR WRINKLES IN ROLLS

The basic geometry under consideration is shown on Figure 1 and it consists of a layer of film under a compressive loading  $F$  in the plane of the film. The lateral support is pictured as an elastic foundation on both sides of the film. This represents all those layers of film above and below the layer in question and is approximated by  $k$ . The basic differential equation describing the displacement of the film layer is derived using this geometry. Here we are looking at a film layer with a radius of curvature which can represent either the circumferential case as it stands or the transverse case with an infinite radius of curvature. The governing differential equation is

$$\frac{d^4 y}{ds^4} + \frac{F}{D} \frac{d^2 y}{ds^2} + \frac{3k}{2D} y = \frac{3F}{2RD} \quad (1)$$

where all variables are defined in the nomenclature (Reference [9] includes a similar analysis for beams).

The solution of the nonhomogeneous form of this differential equation gives rise to the particular solution

$$y_p = F/(kR) \quad (2)$$

which is a form of the belt equation. The buckling analysis depends on the homogeneous portion of the differential equation. Solutions to this portion are based on the characteristic equation where four solutions exist with possible real and imaginary parts. By determining which solutions can achieve a finite displacement  $y$  with only a compressive loading  $F$ , we can establish which represent buckles. Only these buckling modes will be considered in detail.

The first mode of buckling gives rise to a sinusoidal displacement and comes from applying pin-type boundary conditions at both ends of the layer of film. The buckling mode solution for this case is

$$y(s) = C \sin \{ \{3k/2D\}^{1/4} s \} \quad (3)$$

and it is pictured in Figure 2. This type of buckle occurs when

$$F^2/(6 D k) > 1 \quad (4)$$

which is the limiting condition defining the load  $F$  that will cause buckling. The relationship describing the wavelength of the buckle is

$$\Gamma = 2\pi \{2D/3k\}^{1/4} \quad (5)$$

where these relate the wavelength to both the plate stiffness (flexural rigidity) of the film and the radial stiffness,  $k$ , in the roll. These buckling relationships are similar to those obtained by Bang-Eop Lee [10]. Lee solved for the forces required to buckle specific lengths of film. If you solve for the length that coincides with the first mode of buckling in Lee's work and use that length in the force calculation, the results are very similar. However, the typical wavelength is usually much smaller than any roll dimensions. Observations suggest that the buckles form sporadically in the rolls and are not related to any characteristic length of the roll. Buckles form based on their characteristic length and equation (4) will be used to indicate their formation in the winding rolls.

Two other forms of buckles of interest also are described on Figure 2. The first of these is called a transition buckle. It is found by applying a pinned condition at one end and a fixed condition at the other. It represents the transition from flat to buckled film and it requires a higher force to form than the sinusoidal buckling mode. At a slightly higher force  $F$ , a third form of buckle can occur. Unlike the others, it can stand alone as a single, discrete ridge since it has a zero slope at both ends. This one-way buckle comes from a fixed-fixed set of boundary conditions.

Since sinusoidal buckles should occur at lighter loads than a one-way deformation, unique conditions must exist to produce this effect. An example of this type of buckle is the expansion ridges in roads. These almost always are raised ridges since the ground is much stiffer than the air. From this argument and from the buckling force requirements, a second necessary condition for a one-way buckle can be stated as

$$k_+/k_- < 3/50 \quad (6)$$

In words, one-way buckles will only occur when there is a significant difference between the lateral stiffness on the two sides of the layer of film in question. In film winding the one-way buckles generally occur on the roll surface.

The buckles predicted by the theory strongly resemble both machine (MD) and transverse direction (TD) ridges. These sinusoidal ridges are a particular problem in light gage films since thin films have a very low flexural rigidity and are prone to buckling. The MD ridges (tin canning) have a sinusoidal cross section in the transverse direction and, therefore, must be produced by a TD compression. The grooves created by the buckle run around the circumference of the roll and hence the name MD ridges. TD ridges are another form of defect that looks identical to the sinusoidal buckles. This defect is a washboard-like pattern in the single sheet and running across the width of the roll of film. Here, the grooves run in the transverse direction and they are caused by circumferential compression.

The model used here assumes that for the initial deformation the cylindrical shape of a layer of film has no appreciable effect on the formation of a buckle. This is true as long as the radius of curvature is much larger than the film thickness. After the buckle begins to be formed, the magnitude of the deformations become large in comparison to the film thickness and the radius of curvature may influence the shape of the deformation. This often leads to less than perfect TD ridges.

## DERIVATION OF THE ROLL STRESS EQUATIONS

The derivation of the equations describing the formation of stress in a winding roll of film for the plane-strain case parallels that for the plane-stress case in reference

[3]. During this derivation, the strain in the transverse or z direction is set to zero and a relationship for the transverse stress is obtained. The basic differential equation describing the radial stress field for the plane-strain case is

$$\frac{d^2 S_r}{dr^2} + \frac{3}{r} \frac{dS_r}{dr} - \frac{1}{r^2} \frac{E - E_T}{E_T(1-\mu^2)} = 0 \quad (7)$$

The geometry used for this derivation is included as Figure 3. As in the plane-stress analysis, a solution to equation (7) determines the radial stress distribution in the roll produced by applying an exterior wrap of film to the roll (each wrap produces an incremental pressure on the surface of the roll). The final pressure distribution is achieved by summing the stress produced by each layer of film as it is added to the roll. Mathematically this can be stated as

$$P_r(r, R) = \sum_r^R -S_r(r, \delta r) \quad (8)$$

where we sum the stress  $S_r$  produced throughout the roll for each incremental layer of film that is added until the total radius,  $R$ , is reached. This gives the radial pressure distribution. Next, we take the radial distribution and use

$$S_\theta = S_r + r \frac{dS_r}{dr} \quad \text{and} \quad S_z = \mu (S_r + S_\theta) \quad (9)$$

from the derivation of equation (7) to convert to the circumferential and transverse direction stresses. Then a similar summation process is followed as described by

$$P_\theta(r, R) = \sum_r^R -S_\theta(r, \delta r) - S_t(r) \quad (10)$$

$$P_z(r, R) = \sum_r^R -S_z(r, \delta r) \quad (11)$$

Thus, the solution to equation (7) is used to generate the radial, circumferential and transverse direction pressures.

## BOUNDARY CONDITIONS

The roll exterior boundary condition must be applied and modified as the roll builds to reflect changes in tension, radius and any other winding variable that changes. The external pressure is applied by the addition of a differential layer of film as shown on Figure 4. This leads to an external stress given by

$$S_r = (n T_1)/r \quad (12)$$

At the core-roll interface matching conditions are required to establish the stresses at the core surface. This is derived from

$$S_r(R_C^+) = S_r(R_C^-) \quad \text{and} \quad e_\theta(R_C^+) = e_\theta(R_C^-) \quad (13)$$

which come from a summation of forces and geometry considerations, respectively. Reducing this using the basic relationships used to derive equation (7) leads to

$$S_r \left[ \frac{1-\mu-2\mu^2}{E} - \frac{1-\mu_c-2\mu_c^2}{E_c} \right] + r \frac{dS_{r+}}{dr} \left[ \frac{1-\mu^2}{E_c} \right] - r \frac{dS_{r-}}{dr} \left[ \frac{1-\mu_c^2}{E_c} \right] = 0 \quad (14)$$

where the superscripts, + and -, refer to the film and core side of the boundary, respectively. This equation is in a form that can be used with equation (7) to obtain solutions for the incremental stresses both in the film and the core. The boundary condition on the core ID is

$$S_{rC}(R_{ci}) = 0 \quad (15)$$

This boundary condition completes the set required to define the outer surface (12), the core to roll interface (14) and the core ID (15). Solutions to equation (7) are summed as defined in equations (8), (10) and (11) to achieve the total roll stress as the roll builds to completion.

## RADIAL ELASTIC MODULUS FOR FILM AND AIR

The final relationship necessary for the calculation of roll stresses is the radial elastic modulus,  $E_r(P_r)$ . The radial modulus normally is much less than that of the film itself and is dependent on the film surface, film thickness, the amount of entrained air and the pressure in the roll. The basic approach used here was developed by Pfiffer [1,2]. He noted that the stack compression curves for a variety of materials are exponential and can be approximated as

$$P = K_1 \text{EXP}[K_2 e] - K_1 \quad (16)$$

This can be extended to include entrainment effects by defining an initial strain ( $e_1$ ), pressure ( $P_1$ ), air gap ( $h_1$ ) and asperity height ( $h_0$ ) all at the roll surface. Using these terms and assuming an isothermal compression for the air, we get

$$P_r = K_1 \text{EXP}[K_2 (e_r + e_1)] - K_1 + P_1 h_1 / [h_0 - (e_r + e_1)(t + h_0)] \quad (17)$$

and the radial elastic modulus becomes

$$E_r = K_2 K_1 \text{EXP}[K_2 (e_r + e_1)] + P_1 h_1 (t + h_0) / [h_0 - (e_r + e_1)(t + h_0)]^2 \quad (18)$$

This relationship is used for  $E_T$  and is updated after each elemental layer of film is added to the roll surface.  $K_1$  and  $K_2$  can be considered basic film properties and its measurement and relationship to the film surface and thickness are discussed in reference [8]. Determining  $h_1$  and  $P_1$  is discussed in reference [5]. Note that  $h_1$ ,  $P_1$ ,  $e_1$  and film tension  $T_1$  are interrelated by

$$h_1 = h_0 - [(t + h_0)/K_2] \text{Ln} [(K_1 - P_1 + T_1/R)/K_1] \quad (19)$$

and  $e_1 = (h_0 - h_1)/(h_0 + t)$ . Therefore, only the tension and air pressure are necessary to define the conditions at the winding surface.

These same relationships can be used to calculate the internal air pressure between layers of film in the winding roll. Here, the assumption is made that no air leaks out during the winding process. The air pressure under these circumstances is

$$P_a(r, \delta r) = P_1(r) h_1(r)/h = P_1(r) h_1(r)/[h_0 - (e_T + e_1)(t + h_0)] \quad (20)$$

This relationship is used to calculate the air pressure at any time during the film winding.

## EVALUATION OF THE BUCKLING NUMBER

To properly evaluate the tendency to buckle during winding, the loading force and radial stiffness terms in equation (1) must be evaluated throughout the roll as it builds. The loading force is easily determined from equations (10) for TD ridges (TD buckling is induced by circumferential compression) and equation (11) for MD ridges (MD buckling is induced by TD compression). These values are obtained during the solution for the roll stress. The stiffness factor  $k$  is more difficult to obtain. The radial displacement of a layer of film can be determined from

$$q(r, \delta r) = S_r r(1 - \mu - 2\mu^2)/E + (r^2/E) (1 - \mu^2) dS_r/dr \quad (21)$$

This is the amount of displacement of a layer at radius  $r$  due to the addition of an incremental layer of film  $\delta r$  at the surface. The pressure rise at that point that induced the radial motion is  $S_r(r, \delta r)$  and the stiffness factor can be written as

$$k(r, \delta r) = S_r(r, \delta r)/q(r, \delta r) \quad (22)$$

Note that this factor includes the effect of the entire roll and core because it uses the results from the roll stress solution to determine the layer support stiffness.

## SOLUTION METHOD

A finite difference procedure is employed to solve for the roll stresses and a computer program was written. This involved dividing the roll into a number of finite wraps and solving for the incremental pressure rise at each location. The differential equation becomes a set of simultaneous equations of the tridiagonal type which are

solved using a recurrence relationship (see reference [11]). The summations in equations (8), (10) and (11),  $E_r$  and the calculated internal air pressure are updated after each successive layer is added to the roll. Both the applied tension and the entrained air pressure are input as a function of roll radius to reflect the normal variations that occur during winding.

## COMPARISON WITH RESULTS FROM HAKIEL'S WORK

Table 1 includes the data used by Hakiel [3] for calculating winding stresses for a 76 micron (0.003 in) thick polyester film. Calculations using the computer code written for this paper were made to compare with his results. Here, the air portion of the radial stiffness in the roll in the new model has been removed to provide a direct comparison. These results were used to insure the accuracy of the current code and are included on Figures 5 and 6. Figure 5 shows the radial pressure plotted versus roll radius for four cases. Hakiel's results did not include the core thickness and cases were run with the new code and wall thickness' of 6.35mm (0.25 in), 12.7mm (0.5 in) and 22.9mm (0.9 in). The results show that the thickest cases agree almost identically with the Hakiel calculation.

Figure 7 shows the circumferential tension plotted against the roll radius for the same cases. Here, the results from the new code approach the Hakiel results as the core approaches a solid rod.

## TYPICAL RESULTS

A series of test cases were run for the 6 micron film described in Table 2. This relatively thin film was used to demonstrate the use of the buckling criteria described in this paper. Calculated results for this film include (1) the radial stress and (2) circumferential tension both of which are standard results for roll stress. It also includes additional results such as (3) the internal air pressure based on input entrained air pressure, (4) the transverse direction compression introduced by Poisson's ratio effects, (5) buckling number calculations for circumferential compression and (6) buckling number calculations for transverse direction compression.

The first results are shown on Figure 8 where the total radial pressure and the internal air pressure are plotted versus the roll radius. This is for a constant tension winding at 21.5MPa (0.75 pli) with an entrained air pressure of 0.0945 MPa (13.7psia). The shape and magnitude of the total stress are similar to what we would expect based on other calculations and results from experimental measurement. The internal air pressure shows that as the film is compressed during winding the air in the film gaps is also compressed. For the case shown it reaches a value of approximately three atmospheres. This is more than enough to cause leakage of the air from the roll which will result in a shift in the internal stress.

Figure 8 shows results for the circumferential tension and the transverse direction compressive stress. These two variables are plotted on the same graph because they are interrelated. The transverse direction compression is produced primarily by the reduction in tension in the circumferential direction. This is caused, in turn, by the radial displacement of the film layers during winding. It is, as you would expect, approximately equal to the magnitude of the reduction in tension multiplied by Poisson's



ratio (0.4 in this case). The shape and magnitude of the tension curves are as expected and from that it is easy to see that the transverse direction stress has the proper form too. The key areas to look at for buckling are those with compressive loadings in the plane of the film.

The next two plots, Figures 9 and 10, include results for the buckling numbers evaluated for both circumferential and transverse direction compression, respectively. The circumferential buckling number is plotted versus roll radius and it has a positive value only in the region where the tension has been reduced to negative values. The small magnitude of the radial compression results in a small buckling number and this indicates that there will be no buckling due to circumferential compression. This is consistent with experience with this type of film.

Figure 10 shows the buckling number plot for the transverse direction stresses. Here, the transverse direction stresses are higher and the buckling number exceeds one which indicates that buckles will occur. This type of buckle results in "tin canning" or "MD ridges" that run around the circumference of the wound rolls. This is extremely common in rolls of film in this thickness range.

The next three figures include results for a tapered tension case. Here, the initial tension is the same as that for the previous case, 21.5 MPa (0.75pli) but it tapers to 7.18 MPa (0.25pli) at the end of the roll. Figures 11 and 12 include expected results for radial stress, air pressure, circumferential tension and transverse compression. All of these follow expected trends for a tapered tension case. The transverse direction buckling number included on Figure 13 has the key results. It shows that the tapered tension resulted in a lower peak buckling number and it never exceeds one. This result indicates that the film wound with the defined tapered tension will not form MD ridges.

The next two Figures look at an alternate approach to eliminate the buckling for the 6 micron film in question. Here, we are looking at improved air removal by whatever means. The entrained air pressure under these conditions is 0.0807 MPa (11.7psia) or significantly below atmospheric pressure. Figure 14 shows plots of the radial pressure and the internal air pressure for this case. A comparison of the results in Figure 7 shows that the total pressure is slightly higher and that the air pressure is lower. Figure 15 shows the buckling number results for transverse direction compression with the similar results from Figure 7 included for comparison. The tendency to buckle was reduced but the results still indicate that a substantial amount of buckling will occur.

## CONCLUSIONS AND RECOMMENDATIONS

The core material and dimensions can have a substantial effect on the roll stresses near the core. Rather than approximate the core conditions, a complete solution of the winding conditions should include a model of the core itself. This is easily accomplished by using the matching condition in equation 14 and continuing the finite difference approximation through the thickness of the core.

Many of the defects found in wound rolls of film are related to buckling induced by roll stresses. The first mode of buckling that occurs in wound rolls of film has a sinusoidal shape. Stresses exist in wound rolls capable of producing these defects. This characteristic shape is a common defect in wound rolls of thin films (below 25 micron).

The plane-strain approximation gives a more complete picture of the stress in wound rolls. The transverse direction compression is a key to the formation of "tin canning" or "MD ridges" since they are buckles formed by this compression. The

commonly used plane-stress approximation by definition does not determine transverse direction stresses. Plane-strain more accurately depicts the conditions in wide rolls of film where buckling related defects are more common.

The air entrained during winding is compressed to values significantly above atmospheric pressure. A portion of this air will leak out over a period of time and alter the stress distribution in the wound rolls. This is a key cause of defects that form after winding. Calculating the stress distribution in the roll after the air has escaped is the next feature that will be added to our model.

Tapering the tension during winding has a substantial effect on the formation of winding related defects. The tendency for buckles to form increases as the roll radius increases. This is caused by a reduction in the stiffness of the support from the surrounding layers. Here, the core provides the maximum lateral support to the film layers. As the thickness of the layer of film between the core and the point of interest increases, this support drops and buckling occurs at lower compressive loads.

Reducing the pressure of the entrained air by a more effective layon roll system has some advantages. Calculations show that the net effect is a reduced tendency to form winding defects related to buckles. The magnitude of this effect is not as large as using tapered tension for the case considered, however. The observed decrease in the buckling number is related to the fact that the film surface is stiffer than the trapped air. If more of the stress in the wound roll is supported by the stiffer film surface, there is more lateral support for the film layers and a reduced tendency to form buckles. The resulting harder rolls may be subject to other types of defects.

### **BIBLIOGRAPHIC REFERENCES**

1. Pfeiffer, J. D., "Internal Pressures in a Wound Roll of Paper", Tappi, Vol 49, No. 8, pp. 342-7, August 1966.
2. Pfeiffer, J. D., "Predictions of Roll Defects from the Structure Formulas", Tappi Vol 62, No. 10, pp. 83-85, 1979.
3. Hakiel, Z., "Nonlinear Model for Wound Roll Stresses", Tappi, pp. 113-17, May 1987.
4. Struik, L.C.E., "Quarterly Progress Reports Nos. 1 and 2: Film Winding Project", TNO po box 217, 2600 AE delft Netherlands, 1978.
5. Forrest, A. W., "Air Entrainment During Film Winding with Layon Rolls" Proceedings of the Third International Conference on Web Handling, at Oklahoma State University, June, 1995.
6. Forrest, A. W., Letter on Buckling of Laterally Restrained Plates, Sent To: Dr Keith Good of Oklahoma State University, February 20, 1987. (Copies available from author).
7. Good, J. K. and Shelton, J. J., Response Letter to Reference 6 on Buckling of Laterally Restrained Plates, February 1, 1988.
8. Forrest, A. W., "A Mathematical and Experimental Investigation of the Stack Compression of Rough Films", Proceedings of the Third International Conference on Web Handling at Oklahoma State University, June 1993.
9. Allen, T., "One-Way Buckling of Elasticity Restrained Columns", Journal of Mechanical Engineering Studies, Vol 11, No. 3, 1969.
10. Bang-Eop Lee, "Buckling Analysis of Starred Roll Defects in Center Wound Rolls", Ph. D. Thesis at Oklahoma State, May 1991.

11. Richtmeyer, R. D., and Morton, K. W., Difference Methods for Initial Value Problems, Interscience Publishers, New York, pp. 198-201, 1957.

Elastic Modulus of Film	4.13Gpa (600kpsi)
Poisson's Ratio of Winding Roll	0.0
Thickness of Film	76 micron
Outer Radius of Core	25.4 mm (1.0 in)
Outer Radius of winding Roll	76.2 mm (3.0 in)
Elastic Modulus of Core	6.14Gpa
Poisson's Ratio of Core	0
Base Winding Tension	21.5Mpa (0.75 pli)
Radial Elastic Modulus	1060 P - 7.44 X10 <sup>-5</sup> P <sup>2</sup> Pa

TABLE 1. WINDING CONDITIONS AND FILM PROPERTIES FOR HAKIEL COMPARISON CALCULATIONS

Elastic Modulus of Film	3.79GPa (550Kpsi)
Poisson's Ratio of Winding Roll	0.4
Thickness of Film	6 micron
Inner Radius of Core	90 mm (3.54 in)
Outer Radius of Core	100 mm (3.937 in)
Outer Radius of Winding Roll	350 mm (13.78 in)
Elastic Modulus of Core	6.14GPa
Poisson's Ratio of Core	0.4
Maximum Asperity Height	1.5 microns
First Stack Compression Coef. K <sub>1</sub>	2.45KPa (0.356 psi)
Second Stack Compression Coef. K <sub>2</sub>	47.3
Base Winding Tension	21.5MPa (0.75 pli)
Base Entrained Air Pressure	94.5KPa (13.7 psia)

TABLE 2. FILM WINDING CONDITIONS AND MATERIAL PROPERTIES USED FOR CALCULATIONS UNLESS SPECIFIED OTHERWISE

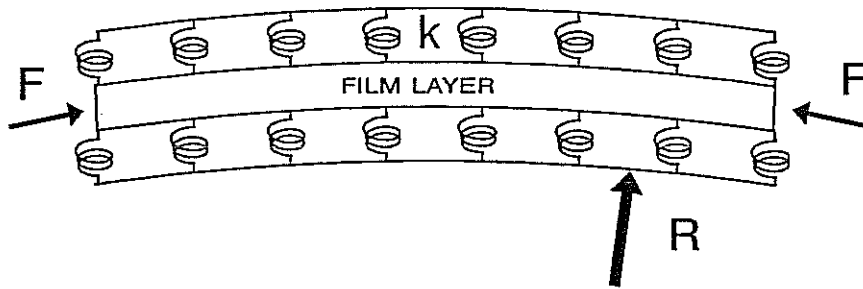


Fig 1 Buckling Theory Model

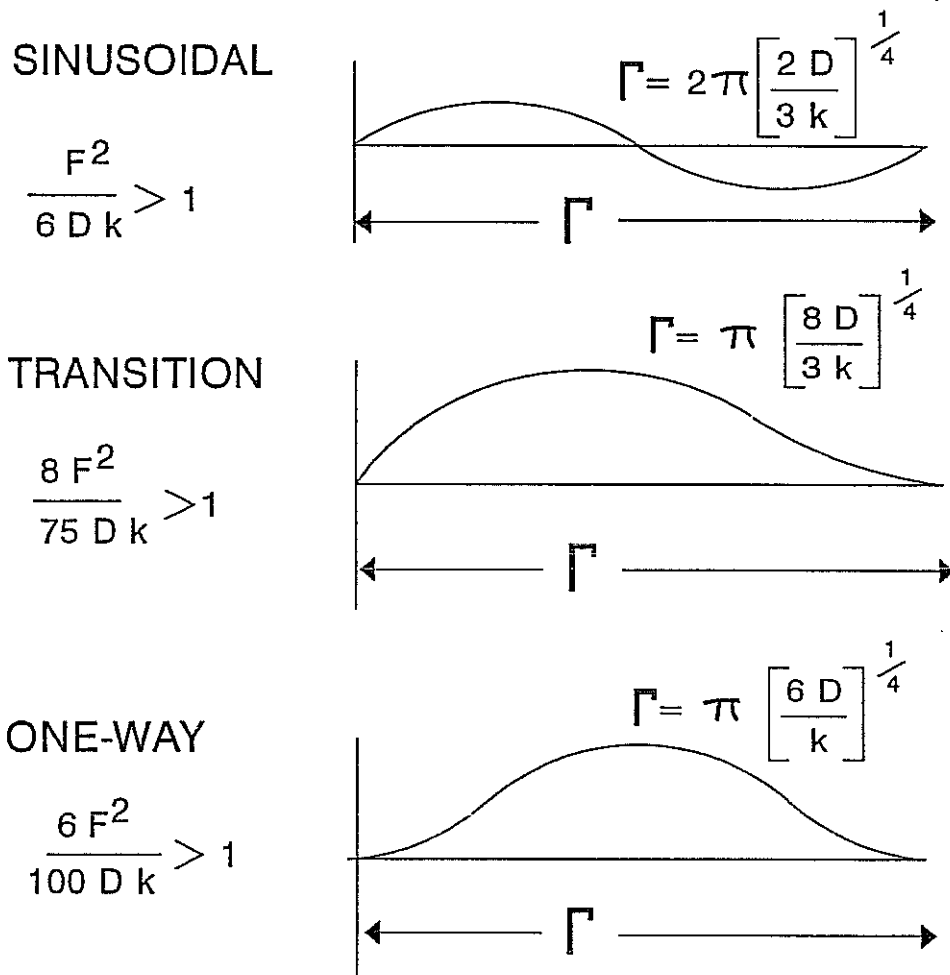
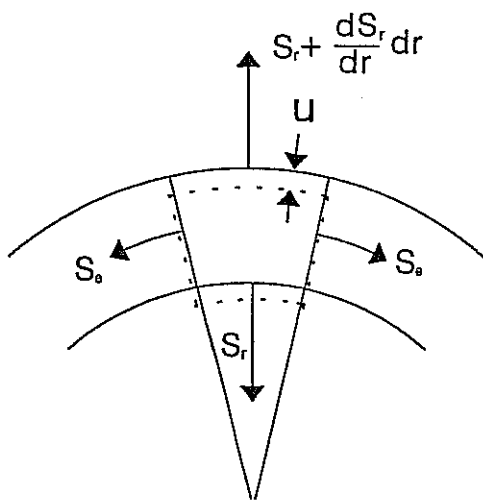


Fig 2 Types and Descriptions of Buckles



RELATIONSHIPS

$$r \frac{dS_r}{dr} - S_\theta + S_r = 0$$

$$r \frac{de_\theta}{dr} = -e_\theta + e_r$$

$$e_r = \frac{S_r}{E_r} - \mu \frac{S_\theta}{E} - \mu \frac{S_z}{E}$$

$$e_\theta = \frac{S_\theta}{E} - \mu \frac{S_r}{E} - \mu \frac{S_z}{E}$$

$$e_z = \frac{S_z}{E} - \mu \frac{S_\theta}{E} - \mu \frac{S_r}{E} = 0$$

Fig 3 Derivation Geometry and Some Basic Relationships

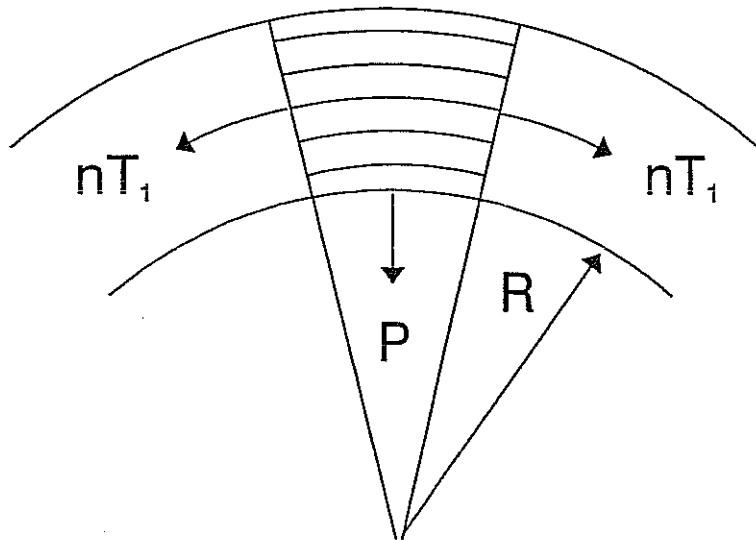


Fig 4 Surface Wrap Boundary Condition Used to Build Winding Rolls

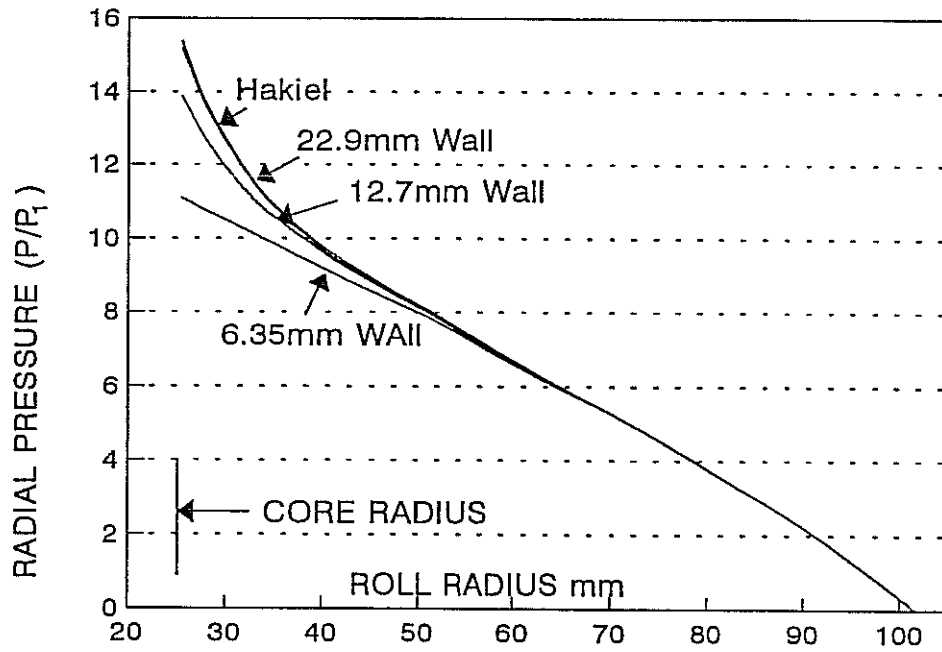


Fig 5 Comparison with Hakiel for 76 micron PET Film Radial Pressure Results

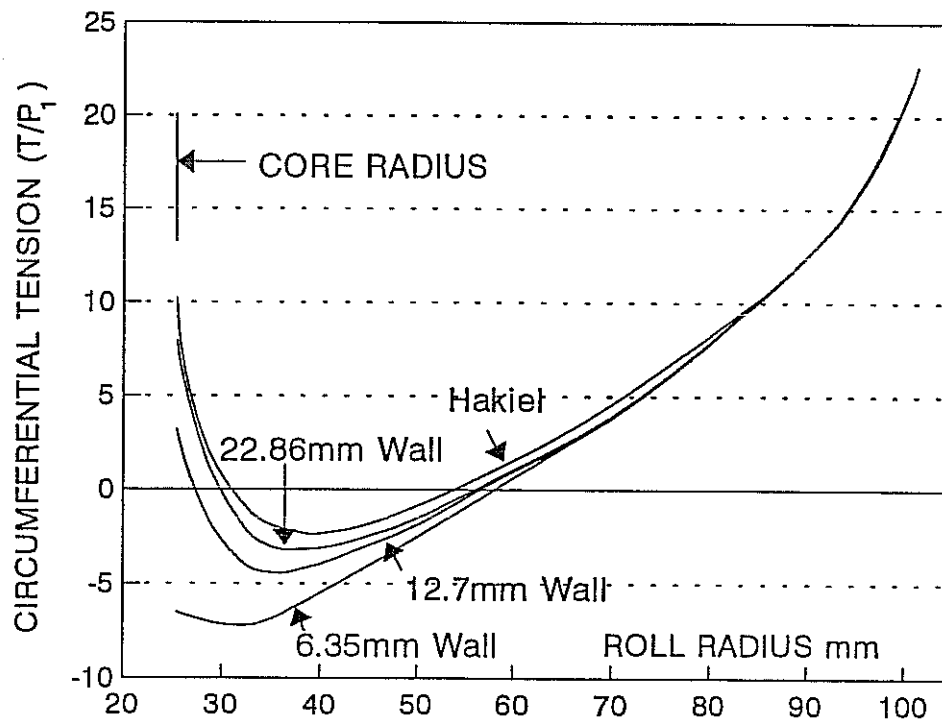


Fig 6 Comparison with Hakiel for 76 micron PET Circumferential Tension Results

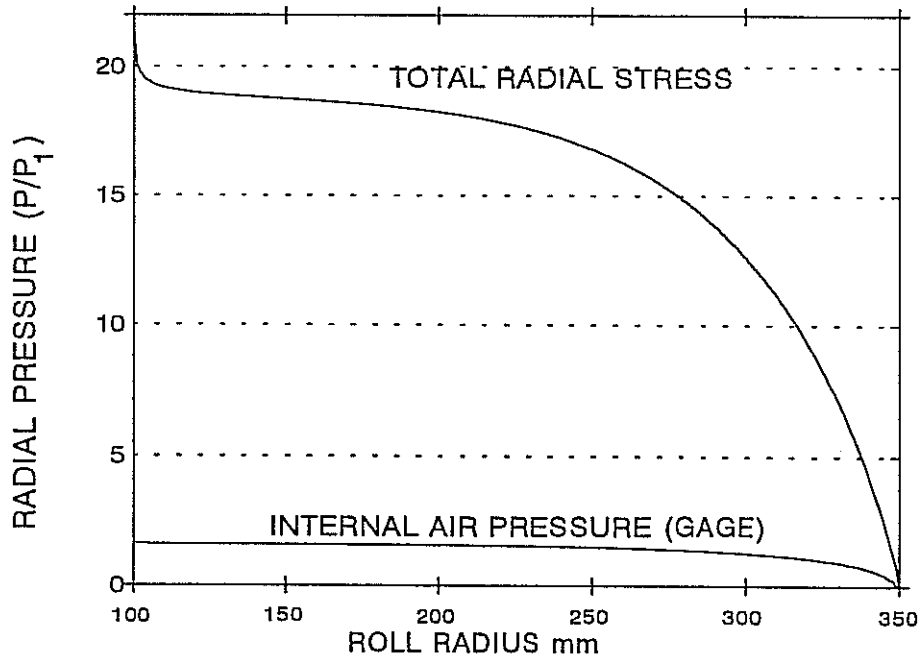


Fig 7 Radial Results for 6 Micron Film Wound at 21.5MPa (0.75pli) with 0.0945MPa (13.7psia) Entrained Air Pressure

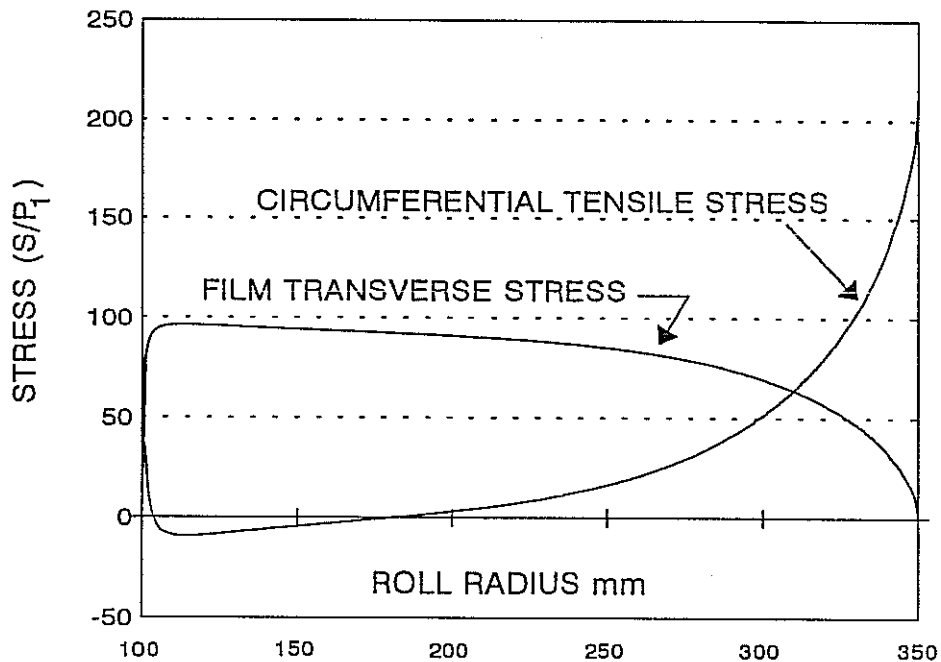


Fig 8 Circumferential and Transverse Stress for 6 Micron Film Wound at 21.5MPa (0.75pli) with 0.0945MPa (13.7psia) Entrained Air Pressure

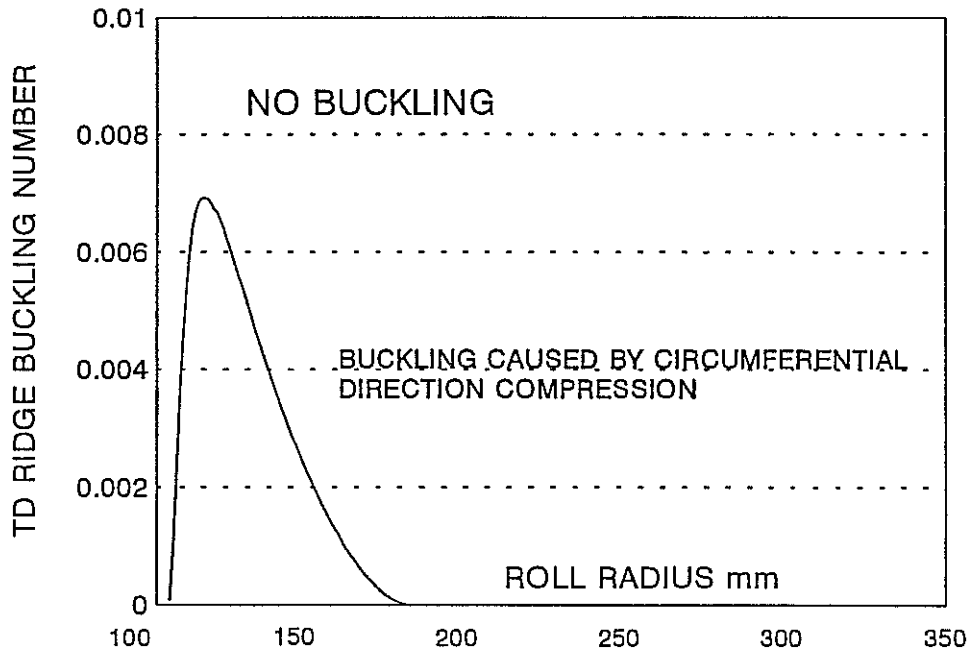


Fig 9 TD Buckling Number for 6 micron Film Wound at a Constant Tension of 21.5MPa (0.75pli) with 0.0945MPa (13.7psia) Entrained Air Pressure

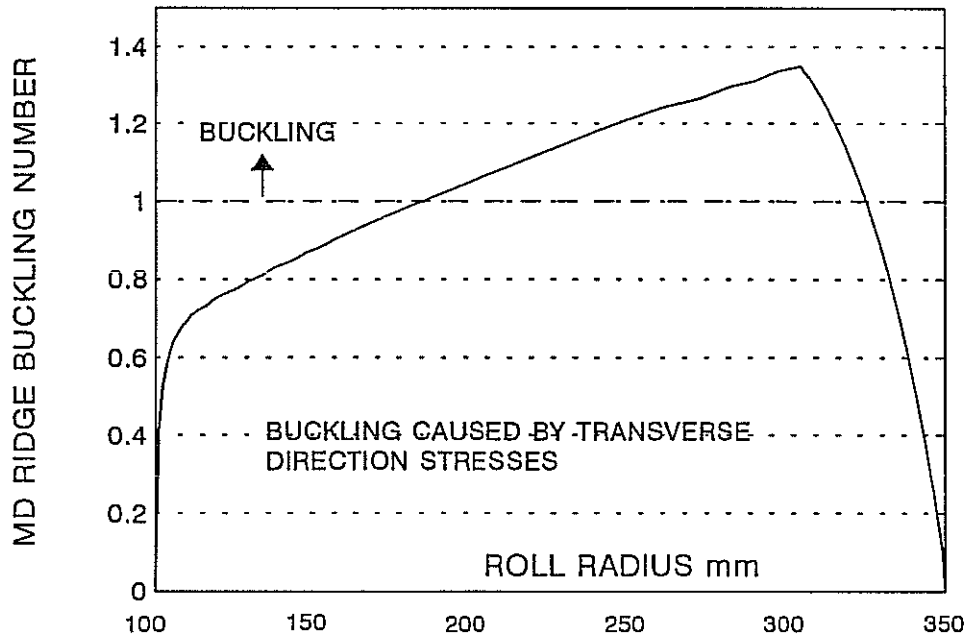


Fig 10 MD Buckling Number for 6 micron Film Wound at a Constant Tension of 21.5MPa (0.75pli) with 0.0945MPa (13.7psia) Entrained Air Pressure



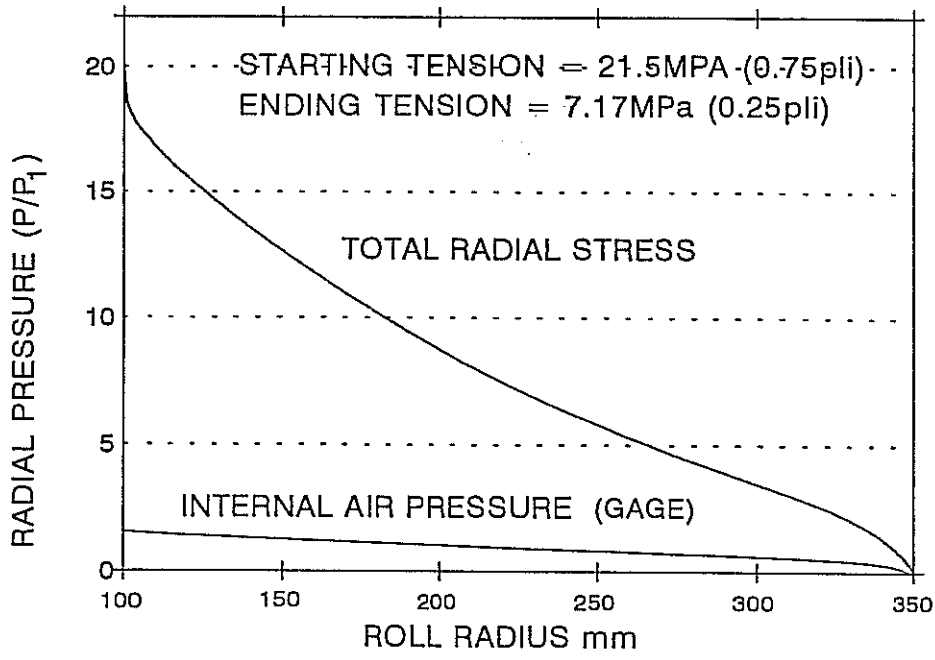


Fig 11 Radial Results for 6 Micron Film Wound Using Tapered Tension with 0.0945MPa (13.7psia) Entrained Air

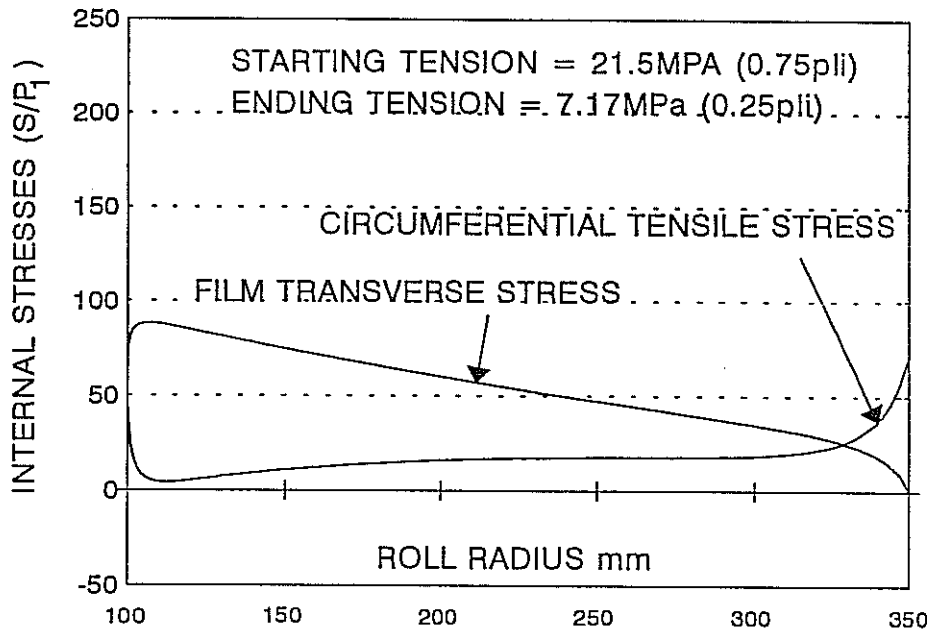


Fig 12 Circumferential and Transverse Direction Results for 6 Micron Film Wound Using Tapered Tension with 0.0945MPa (13.7psia) Entrained Air

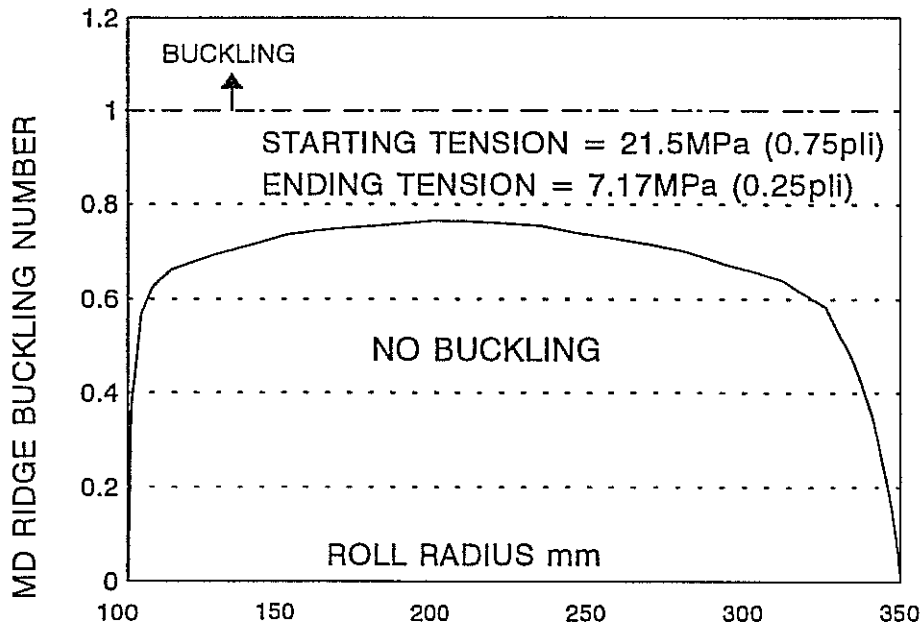


Fig 13 MD Buckling Number for 6 micron Film Wound with a Tapered Tension with 0.0945MPa (13.7psia) Entrained Air Pressure

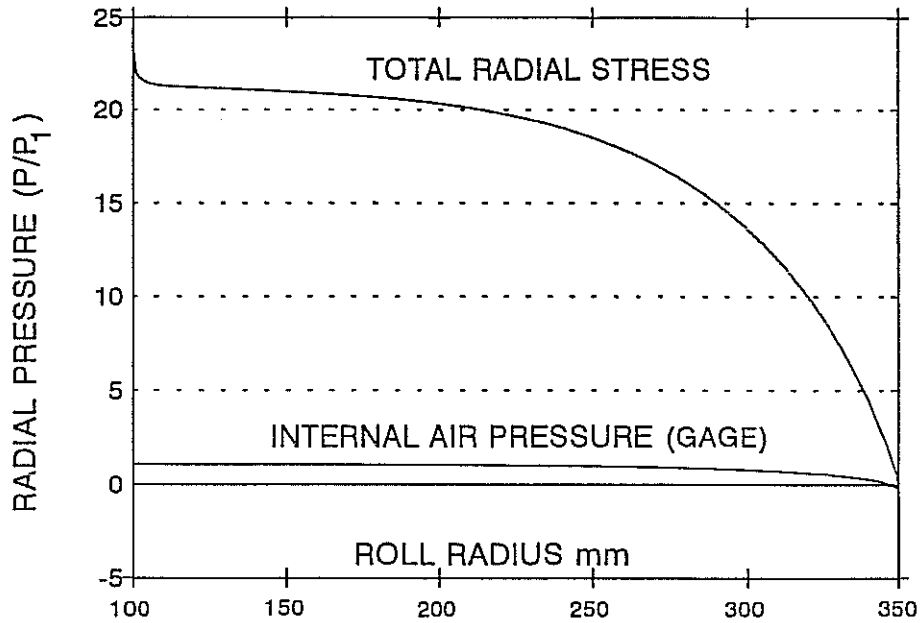


Fig 14 Radial Results for 6 micron Film Wound at 21.5MPa (0.75pli) with 0.0807MPa (11.7psia) Entrained Air Pressure

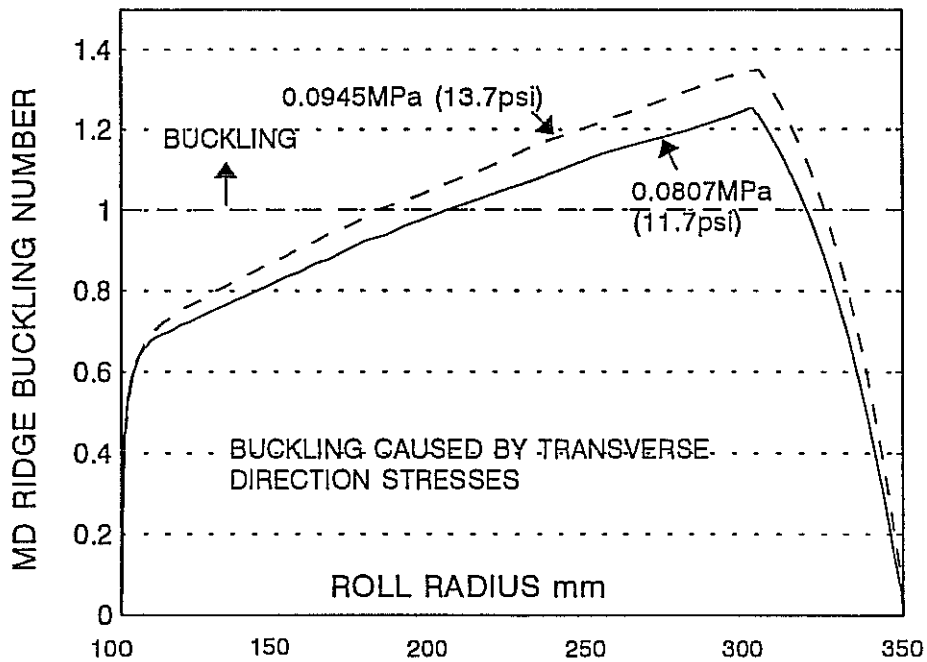


Fig 15 MD Buckling Number for 6 micron Film Wound at 21.5MPa (0.75pli) with 0.0807MPa (11.7psia) Entrained Air Pressure

Forrest, A.W.

Wound Roll Stress Analysis Including Air Entrainment and the Formation of Roll Defects

6/19/95 Session 2 2:00 - 2:25 p.m.

Question - Your model seems to indicate the characteristic length of the buckling which is the function of stiffness and the film thickness. I think there is a lot of work showing that the roll diameter plays quite a large part and the wave length is proportional to the square root of the roll radius times the thickness. Would you care to explain that.

Answer - In the range where we have the ridges, for example, you might be talking more of the circumferential buckle, starting type of effect. Which are you referring to the starting or MD ridges? (Tin Canning?)

Question - MD ridges which go around the circumference.

Answer - We have not noticed that, to be honest with you.

Question - A quick clarification, the Poisson's ratio 0.4 that you use for PET, is that the portion of the bulk material that you use in your  $E_r$  expression for the actual roll winding model, or is that just the portion ratio for PET itself.

Answer - That is PET, in the film itself.

Question - So for the winding model your effective portion ratio was 0 or close to 0.

Answer - No I don't think so, it's 0.4, but you need to make sure you don't get it confused with the  $E_r$ .

Question - My only point is that most authors in the past have used the portion ratio close to 0 for their winding model.

Answer - The measurements we've made for our Poisson's ratio for PET films is around 0.4.

Question - In the stack compression tests.

Answer - No, No.

Question - Just in the film.

Answer - In the film.

Question - OK

Answer - OK

Question - That too was my question, what few measurements I have made on Poisson's ratio that would say couple a radial and axial deformation through the roll. I found it to be in very few small numbers just like Hakiel and others found for  $E_r$  data quite small compared to 0.4 anyway.

Answer - I think it does approach the bulk value after the film has blocked or what we call blocking where the film is run together.

Question - The majority of the effect of the portion ratio to generate the transfer stress comes from the  $\mu$  times the sigma or the tensile stress in the film. This (the radial portion) is a small portion of it.

Answer - Yes I would like to discuss that further with you, but the majority of the stress that comes in for the transverse direction compression that give rise to the tin canning is  $\mu$  times the tension that's relaxed down.

Thank you.